Thermal Insulation Performance Optimization of Hollow Bricks Made up of 3D Printable Rubber-Cement Mortars: Material Properties and FEM-based Modelling

Thermal Insulation Performance Optimization of Hollow Bricks Made up of 3D Printable Rubber-Cement Mortars: Material Properties and FEM-based Modelling

M Sambucci[1,2,*] **and M Valente**[1,2]

[1] Department of Chemical and Material Engineering, Sapienza University of Rome, 00184 Rome, Italy
[2] INSTM Reference Laboratory for Engineering of Surface Treatments, Department of Chemical and Material Engineering, Sapienza University of Rome, 00184 Rome, Italy

[*] matteo.sambucci@uniroma1.it

Abstract. Sustainable construction is attracting more attention lately. It involves the design of eco-friendly building structures, the reduction of energy consumption and waste, the use of renewable and recyclable resources, and the enhancement of low-impact manufacturing methods. This paper addresses some of these sustainability questions, in the context of the use of tire recycled rubber particles as aggregates of cement mortars suitable for Additive Manufacturing (AM) processes. Specifically, the effect of rubber aggregates on physical and thermal properties was investigated, to evaluate the heat-insulating performance of the compounds. The lightweight and non-polar nature of rubber improve the thermal insulation and physical-structural properties of the material, in terms of thermal conductivity, unit weight, and porosity respectively. However, these effects are closely related to the particle size and their adhesion with the cement matrix. In the second part of the manuscript, applicability study of rubber-cement compounds based on the design and finite element method (FEM)-based thermal analysis of innovative hollow bricks is presented. Fractal cavities were investigated as a functional inner architecture to improve the thermal behavior of the component. FEM results show an increase of more than 30% in thermal resistance (R_T) for fractal-based brick compared to conventional designs, demonstrating that the holes' geometric irregularity is a key feature in the thermal flow attenuation.

1 Introduction

Brick is one of the main building materials of masonry structures. Since the ancient Romans period, no other material has managed to replace it, due to its durability, insulating power, cheapness, and mechanical strength. Nowadays, the rising demand for building materials, the increase in demolition wastes, and the impact of brick manufacturing processes on the environment and human health have encouraged the development of sustainable architecture and construction [1]. These approaches are focused on the design of structures and architectural units with low environmental impact, minimizing the use of natural resources, and enhancing energy efficiency. In this framework, the use of industrial wastes as aggregates of cement mortars can represent a noteworthy strategy in terms of sustainability and functional properties. In the literature, several examples on the reuse of recycled fillers in cementitious compounds can be found, including PET particles [2], wood chips [3], glass powder [4], and waste tire rubber aggregates (TRA) [5]. The reuse of shredded TRA as building materials constituents is a widely studied solution by researchers to counteract the environmental pollution,

accumulation of end-of-life tires, and to design lightweight materials with improved ductility, durability, and thermo-acoustic insulation properties [6,7].

This work focuses on the experimental studies related to the development of technologically advanced cementitious mortars suitable for Additive Manufacturing (AM) process modified with polymer particles deriving from waste tires. The possibility of using the rubberized compounds in 3D printing technology represents the novel aspect of this research. As well investigated, AM in the construction sector implies interesting benefits [8]: a) building materials savings and demolition wastes reduction; b) lowering in injury rates; c) high architectural flexibility. According to the requirements mentioned above, an attractive perspective opens up in the design of more eco-friendly and engineering-functional building components.

To investigate the peculiarities of these mixtures as insulation solutions in the construction field, the effect of tire rubber on thermal performance was analyzed by physical and thermal experimental testing. First, three different printable rubber-cement compounds (100 % sand-rubber replacement level) varying the size of TRA (0-1 mm rubber powder and 2-4 mm rubber granules) were studied. Control mortar (CTR) containing 100 % sand was also prepared to compare its properties with those of rubber-modified samples. Finally, the authors present a Finite Element Method (FEM)-based thermal analysis on the technological applicability of these materials for the manufacturing of multi-perforated bricks. Specifically, different hole designs were examined and then evaluated the heat insulation performance of the bricks in terms of thermal resistance (R_T). Innovative inner architectures based on hexagonal and fractal cavities were investigated and compared with conventional configurations. As suggested by a previous analytical study [6], hexagonal cells improve the mechanical deformability behavior and the sound insulation performance of the brick, maintaining satisfactory structural properties. On the other hand, fractal cavities could represent an ideal candidate for the thermal optimization of bricks, due to the marked geometry complexity. As confirmed by Bustamante et al. [9], the increase in the shape complexity of the holes improves the thermal behavior of hollow blocks, because the thermal trajectory is maximized and therefore the convection heat transfer is reduced. The research's purpose is to obtain a "bifunctional" building element, having optimized insulating properties deriving both from the material composition and its topological features.

2. Materials and Methods

2.1. Materials
3D printable rubber-cement mixtures were obtained starting from a control mortar (CTR) consisting of Type I Portland cement, limestone sand of 0.4 mm nominal maximum size, and a specific blend of chemical additives (Silica fume-based thixotropic additive, Polycarboxylate ether-based superplasticizer, Aliphatic-based water reducing agent, and Calcium oxide-based expansive agents). Two type of TRA from the mechanically grinding process of waste tires, sourced by European Tyre Recycling Association (ETRA), were used as a total replacement of sand by volume: 0-1 mm rubber powder (RP) and 2-4 mm rubber granules (RG). The average density of rubber aggregates, evaluated by Micromeritics AccuPyc 1330 He-pycnometer, is 1202 kg/m^3. By varying the replacement ratios of RP and RG, three rubberized mortars were developed and tested.

As shown in table 1, water dosage is the only parameter that is altered in the mixes production. The proper mixes rheology was selected following specific printability requirements [8]: extrusion process without interruptions (*extrudability*), stacking integrity between printed layers (*buildability*), and strong layer-by-layer binding (*inter-layers adhesion*). These 3D printing indicators were evaluated by printability tests described in the next section.

Table 1 presents the mix compositions for CTR mix and rubber-cement compounds per m^3.

Table 1. Mix proportions for CTR and rubberized mortars

Mix design	CTR	RP100	RP50RG50	RP25RG75
RP content [% v/v]	0	100	50	25
RG content [% v/v]	0	0	50	75
Cement [kg]	800	800	800	800
Water [kg]	300	260	250	230
Sand [kg]	1100	0	0	0
RP [kg]	0	300	150	75
RG [kg]	0	0	160	240
Additives [kg]	152	152	152	152

2.2. Printability test and specimens manufacturing

Printability tests were conducted to evaluate the print quality of the mixtures investigated in this research. For this purpose, a COMAU 3-axis robotic arm-based printing apparatus equipped with a circular nozzle (Ø = 10 mm) was adopted. Dry components were mixed in an Aluminum tank for 45 s. Water was then added to the dry compound and mixed for 12 min with an electric mixer drill. After this, the fresh material is deposited in the delivery system for printing. The extrusion speed and the deposition pressure were fixed at 33 mm/s and 4 bar, respectively. Six-layers slabs (230 mm x 160 mm x 55 mm) were printed using each mixture to test the extrudability, buildability, and inter-layer adhesion requirements. Specimens used for the thermo-physical characterization of the materials were extracted from these printed structures by sawing with a diamond blade. Specifically, four blocks with dimensions 48 mm x 42 mm x 22 mm for each mix were used for laboratory testing. After extraction, a lapping treatment was performed on the specimens, using a Buehler 180 grit carbide abrasive disk, to obtain flat and regular faces. The stages related to the specimens manufacturing are summarized in figure 1.
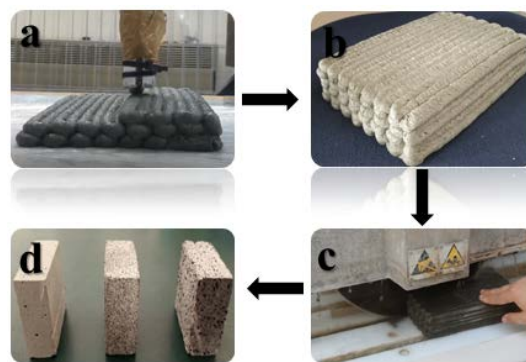
Figure 1. Specimens manufacturing process: printability test (a), slabs manufacturing (b), slabs cutting (c), and post-lapping samples (d).

2.3. Laboratory tests

Density, porosity, and heat transfer properties are key physical quantities to describe the thermal behaviour of the materials. In this regard, a series of laboratory tests were conducted to evaluate the effect of TRA on the thermo-physical properties of the cement-based compounds. Furthermore, the

experimental results were used as input data for the FEM-based thermal analysis on the hollow bricks optimization described below.

The bulk density (ρ_b) of the samples was determined by the mass and volumes of the oven-dried blocks (110 °C for 48 h) in accordance with BS 1881-114 standard [10].

Vacuum saturation technique, as described in ASTM C1202 [11], was conducted to evaluate the permeable porosity (φ). The sample weight was measured after three physical treatments: 1) oven treatment (110 °C for 2 h); 2) vacuum saturation treatment (0.3 bar for 3 h); 3) water saturation treatment (underwater soaking for 24 h). φ was computed considering the weight gain due to water absorption. In support of φ measurements, the microstructure and pore distribution of the samples were inspected by microscopy analysis using a Leica MS5 stereomicroscope.

Thermal transport properties of CTR and rubberized specimens, including thermal conductivity (k) and heat capacity (C_p), were measured using a C-Therm TCi Thermal Conductivity analyzer (figure 2). According to Modified Transient Plane Source (MTPS) method (ASTM D7984) [12], a one-sided thermal sensor applied a low energy current pulse for 0.8 s to the specimen, so that the k measurement was not affected by thermal convection. Some of the generated heat is absorbed by the specimens and the remaining part is used to increase the temperature at the sensor-sample interface. The temperature variation implies a resistance change of the sensor, resulting in a voltage drop. Voltage data is used to evaluate the thermal transport properties of the investigated material. k and C_p results were obtained from 5 averaged measurement in each mix.


Figure 2. Thermal characterization of rubber-cement samples: C-Therm TCi analyzer (a), and test configuration (b).

2.4. FEM-based thermal analysis on rubber-cement hollow bricks

Hollow bricks are energy-efficient building components because of their combined lightweight, deformability, thermal capacitance, sound insulation, and durability [6]. To reduce the energy consumption and improve the safety and comfort of the structures, a number of studies in the building and architectural fields have focused on increasing the performance of construction components and units. Thanks to the development of FEM techniques and advanced manufacturing methods (such as AM), topological optimization can be considered a valuable approach to model and prototype building elements, having a functional design. As suggested by some researches [9,13], by varying the cavity shapes of a brick its thermal inertia can be modulated. However, traditional manufacturing techniques do not ensure great design freedom and therefore the applications in this regard are very limited. On the other hand, combining AM with cementitious materials is an attractive approach to broaden research and studies on shapes and geometries with improved engineering functionality.

In this manuscript's section, the authors present an applicability study of rubber-cement mixtures for the development of hollow bricks with innovative inner designs. Specifically, the thermal insulation behaviour of bricks based on hexagonal and fractal geometry cavities was simulated and compared with common brick designs.

2.4.1. Bricks geometry.
The FEM-based investigation of R_T of hollow bricks was performed on 6 three-dimensional models. The prototypes had the same external dimension (250 mm x 150 mm x 55 mm) and hole concentration ratio (~ 40 %), but different inner design. The top views of the brick models are shown in figure 3.
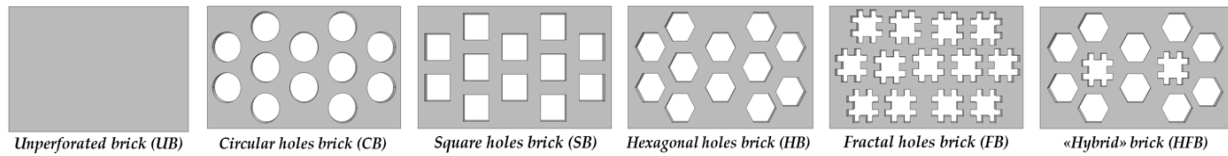
Figure 3. Design of the multi-holed bricks

UB identified the unperforated block. CB model is composed of circular holes with 13 mm radius. In SB block, the side of the squares is 33 mm. The hexagons side in HB model is 20.5 mm. The edge of the fractal structures in FB brick is 8 mm. Finally, HFB combined block consisting of an array of 10 hexagonal holes containing two fractal cavities, was tested.

2.4.2. FEM model for heat transfer in hollow bricks. FEM-based analysis on the thermal performance of the brick prototypes was performed using the Heat Transfer in Solids Module of COMSOL Multiphysics 5.4 software. R_T was determined through steady-state thermal analysis, as suggested by ISO 9869 standard. The procedure involves the application of temperature gradient (ΔT) across two brick faces perpendicular to a spatial direction, keeping the other boundaries in thermal insulation condition (no heat flux across the surface). These temperatures comply the average summer and winter climatic conditions in Italy and accurately reproduce the environmental circumstances to which the building elements are subjected. In summer conditions, the outdoor (T_{out}) and the indoor (T_{in}) temperatures were set equal to 40°C and 26°C, respectively. In winter conditions, T_{out} and T_{in} were fixed to 0°C and 20°C, respectively. Besides, the same values of heat flux coefficients were used in both summer and winter states, due to the negligible divergence ($\sim 3\%$) in the two investigated climatic circumstances. Outdoor heat flux coefficient (h_{out}) and indoor heat flux coefficient (h_{in}) were set equal to 24 W/m²K and 7.69 W/m²K, defined by ISO 6946 method. To improve the FEM study, additional thermal ambient properties were selected: average wind velocity (v_w), clear sky normal irradiance (I_{sn}), and clear sky diffuse irradiance (I_{sd}). v_w was taken to be 3.6 m/s [14]. Summer and winter I_{sn} were set as 236 W/m² and 64 W/m², respectively. Summer and winter I_{sd} were fixed equal to 93 W/m² and 28 W/m², respectively. Irradiance data were deduced by [15], averaging the experimental values, measured in Italy, in summer (May, June, July, and August) and winter (November, December, January, and February) periods. FEM simulation is based on the application of a convective heat flux density on the outdoor (q_{in}) and indoor (q_{out}) faces of the brick (W/m²). Indoor and outdoor heat flows extracted by convection follows Newton's law of heat (1,2):

$$q_{in} = h_{in} \times \left(T_{in} - T_{if} \right) \tag{1}$$

$$q_{out} = h_{out} \times \left(T_{out} - T_{of} \right) \tag{2}$$

where T_{if} and T_{of} are the indoor and outdoor boundary surface temperatures (K), respectively. In steady-state condition, the heat exchange and transmission processes are governed by the thermal Ohm's law (3), which state that the thermal power Q (W) is directly proportional to the temperature gradient ($T_{if} - T_{of}$) causing the thermal exchange:

$$Q = \frac{A}{R_T} \times \left(T_{if} - T_{of} \right) \tag{3}$$

where A is the cross-sectional area perpendicular to the path of heat flow (m²). R_T (m²K/W) is strongly related to the thermal inertia of the bricks, which depends on the specific heat capacity, the thermal conductivity, and density of the material. The configuration for thermal simulation of hollows bricks performance is presented in figure 4.
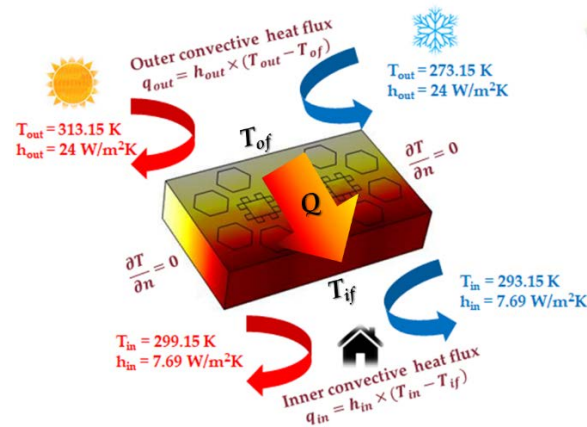
Figure 4. FEM-based thermal analysis: simulation configurations

By using Q, T_{if}, and T_{of} calculated through the software, it is possible to estimate the R_T of the bricks.

2.4.3. Materials and meshing. Hollow brick models are composed of two domains: solid material and cavity. For the solid domain, the thermo-physical properties (ρ_b, φ, k, and C_p) of the cement mixtures evaluated in the experimental tests were set. The holes were simulated as air domains by setting the fluid properties from the COMSOL materials library. A fine free-tetrahedral mesh (maximum element size of 20 mm) was used to discretize the entire model

3. Results and Discussions

3.1 Thermo-physical properties of rubber-cement mortars
Generally, density and porosity of cementitious materials depend on the aggregate unit weight of aggregates, size of dry constituents, entrapped air, water-cement ratio, and aggregate-cement paste adhesion. As shown in table 2, replacing sand with tire rubber-based lightweight aggregates implies a reduction in ρ_b and φ of the cement mortar.

Table 2. Density and porosity of mortars with aggregates replaced by rubber particles

Sample	ρ_b (kg/m^3)	ρ_b reduction (%)	φ(%)	φ reduction (%)
CTR	1927	/	33.1	/
RP100	1340	- 30.5	22.1	- 33.2
RP50RG50	1624	- 15.7	26.1	- 21.1
RP25RG75	1468	- 23.8	25.7	- 22.4

Changing of physical properties is also due to the rubber particles' tendency to entrap air in their rough surface, as a consequence of their hydrophobic features. However, the non-polar nature of TRA affects the rheological properties of the mixtures. As reported in Table 1, the rubberized compounds consist of lower water dosages than the CTR mix, resulting in lower capillary porosity and air bubbles fraction [16]. This is verified by microstructural analysis, using optical stereomicroscope, reported in figure 5.
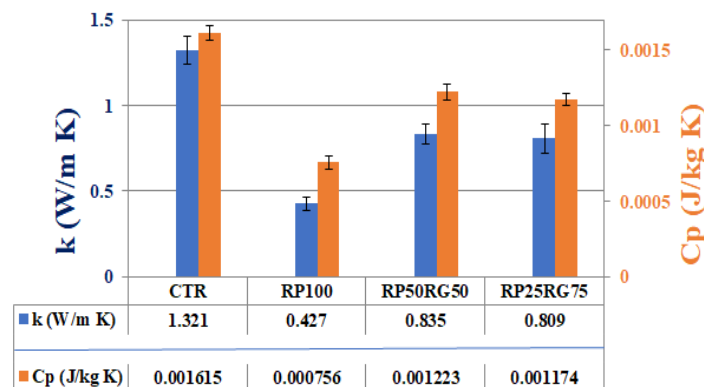
Figure 5. 16x magnification optical micrographs of printed samples

By comparing the rubberized mixes behavior, the reduction rates follow a very random trend. Indeed, several competitive factors affect the physical properties of the compounds: a) the effective amount of rubber incorporated into the material; b) the different air adsorption tendency of TRA; c) the rubber-cement adhesion properties. Due to a high specific surface, RP promotes better cohesion with the cement paste but exhibits a greater aptitude for incorporating air. RG allow keeping the water-cement ratio at a low level, hindering the formation of capillary porosity. However, they promote the formation of interface voids due to poor bonding with the matrix [6,7].

Thermal characterization results, given in figure 6, show that the addition of TRA considerably reduce the k-value of the rubber-based mixtures. This decrease is mainly attributable to the higher thermal insulation behavior of the rubber particles than mineral aggregates. Besides, the ability of TRA to entrap air and the material's interfacial porosity are beneficial to obtain low heat conductivity. Due to the relevant thermal inertia of the air, voids oppose the thermal transfer through the matrix, reducing the thermal bridge effects [17]. According to the technical indications given by Newman and Owens [18], rubberized mortars can be classified as lightweight insulating cement materials: oven-dry density range of approximately 300 to a maximum of 2000 kg/m^3 and k-value of 0.2 to 1.0 W/m K.

	CTR	RP100	RP50RG50	RP25RG75
k (W/m K)	1.321	0.427	0.835	0.809
Cp (J/kg K)	0.001615	0.000756	0.001223	0.001174

Figure 6. k and C_p experimental results

Finally, it is possible to observe that k and C_p varied in the same direction. This is agreeing well with the direct proportionality between the two thermal quantities, well highlighted in the following equation (4):

$$C_p = \frac{k}{\rho_b \times \alpha} \tag{4}$$

where α is the material diffusivity (m^2/s).

3.2 Thermal performance of rubber-cement brick model: FEM analysis results
R_T is one of the key parameters to analyze the response of a building structure to specific environmental conditions and therefore evaluate its energy performance [14]. The results obtained using FEM are processed in order to obtain the overall R_T for each type of brick design and printable cement mortar (figure 7). The calculation of this parameter was performed in the summer and winter

conditions discussed above. The analytical data, determined in the two environmental states, were averaged to provide univocal R_T-value.
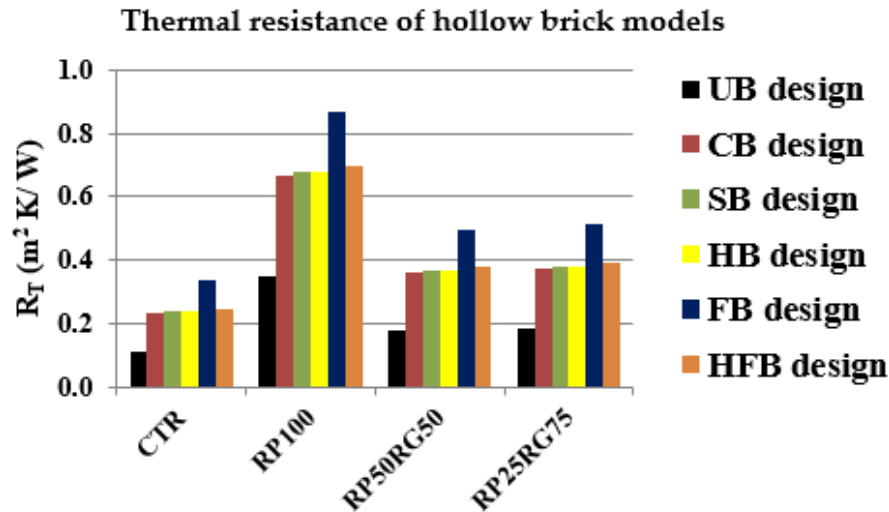
Figure 7. FEM results for the rubber-cement bricks of the overall R_T

Three relevant results can be deduced from the numerical thermal analysis:
1. Regardless of brick design, R_T is closely related to the heat-insulating properties of the material. The highest R_T-values are observable for RP100 mix, where lower k-values were experimentally found compared to the other printable mortars.
2. As expected, inner holes significantly improve the thermal insulation performance of the component. By considering perforated models, it is possible to observe R_T-values up to three times higher than UB design, depending on the hollow architecture and cement material. The air cavities act as high-thermal inertia sites, opposing the thermal flow through the material, and enhancing its R_T.
3. In each cement compound, R_T performance of FB design is the best. As reported in [6,9], the high geometric complexity of the inner cavities maximizes the thermal path of heat flow, resulting in greater thermal attenuation than conventional architectures. *FB* brick implies a 37%, 34% and 35% average increase in R_T over the CB, SB, and HB models, respectively. However, the fractal cavities morphology may not be optimal in terms of structural performance, since the small curvature radius zones represent preferential triggering points for structural cracks when the brick is subjected to mechanical load. To compensate this potential structural weakness, the authors propose HFB geometry that combines the mechanical-acoustic efficiency of hexagonal holes with the thermal performance of the fractal ones. As know, hexagonal architectures are efficient structures for bending stiffness, due to their aptitude to dissipate residual mechanical stress under load [6]. As shown in figure 7, better thermal insulation response is observed for the hybrid design than conventional geometries, resulting in a potential good matching between structural and thermo-acoustic properties.

4. Conclusions and future work
In the first part of this research work, the thermo-physical performances of 3D printable tire rubber-cement mortars were studied. Rubberized mixtures exhibit superior lightweight, microstructural, and thermal insulation properties than plain cement sample as measured by the decrease in density (ρ_b), porosity (φ), and thermal conductivity (k) values, respectively. The percentage-wise improvements on insulation, porosity degree, and unit weight are strictly dependent on the non-polar nature and size of the polymer aggregates that replace the sand. Finally, a numerical thermal analysis technique (FEM)

was employed to perform an optimization design study on rubber-cement hollow brick prototypes. To improve the thermal resistance (R_T) of building components innovative inner designs based on fractal and hexagonal cavities were tested. Fractal holes-based brick (FB) shows optimum thermal behavior compared to conventional architectures. Due to its geometrical complexity, fractal cavities maximize the thermal trajectory of the heat waves causing relevant attenuation. Hybrid design (HFB) shows intermediate thermal insulation performance between FB and conventional designs but could be more efficient in terms of mechanical properties. Future researches will be focused on evaluating the feasibility in bricks AM, validating the numerical results with laboratory tests, and conducting further studies (FEM and experimental) on the mechanical and acoustic performance of the models.

Acknowledgments

References

[1] Petrillo A, Cioffi R, Ferone C, Colangelo F and Borrelli C, Eco-sustainable geopolymer concrete blocks production process 2015 *Agriculture and agricultural science procedia* **8**(8) 408-18

[2] Saikia N and de Brito J., Mechanical properties and abrasion behaviour of concrete containing shredded PET bottle waste as a partial substitution of natural aggregate 2014 *Construction and building materials* **52** 236-44

[3] Corinaldesi V, Mazzoli A and Siddique R, Characterization of lightweight mortars containing wood processing by-products waste 2016 *Construction and Building Materials* **123**, 281-89

[4] Du H and Tan K H, Properties of high volume glass powder concrete 2017 *Cement and Concrete Composites* **75** 22-29

[5] Siddika A, Al Mamun M A, Alyousef R, Amran Y M, Aslani F and Alabduljabbar H, Properties and utilizations of waste tire rubber in concrete: A review 2019 *Construction and Building Materials* **224** 711-31

[6] Valente M Sambucci M, Sibai A and Musacchi E, Multi-Physics Analysis for Rubber-Cement Applications in Building and Architectural Fields: a Preliminary Analysis 2020 *Sustainability*, **12**(15) 5993

[7] Sambucci M, Valente M, Sibai A, Marini D, Quitadamo A and Musacchi E 2020 Rubber-Cement Composites for Additive Manufacturing: Physical, Mechanical and Thermo-Acoustic Characterization 2020 In *Bos F., Lucas S., Wolfs R., Salet T. (eds) Second RILEM International Conference on Concrete and Digital Fabrication. DC 2020*. RILEM Bookseries, vol 28. Springer, Cham

[8] Valente M Sibai A and Sambucci M, Extrusion-Based additive manufacturing of concrete products: Revolutionizing and remodeling the construction industry 2019 *Journal of Composites Science* **3**(3) 88

[9] Bustamante W, Bobadilla A, Navarrete B, Vidal S and Saelzer G. Thermal improvement of perforated ceramic bricks 2009 *Revista de la Construcción* **8** 24-35

[10] British Standards Institution. BS 1881-114: Testing concrete. Method of determination of density of hardened concrete-1983

[11] American Society for Testing and Materials. ASTM C 1202: Standard Test Method for Electrical Indication of Concrete's Ability to Resist Chloride Ion Penetration-2002

[12] American Society for Testing and Materials. ASTM D 7984-16: Standard Test Method for Measurement of Thermal Effusivity of Fabrics Using a Modified Transient Plane Source (MTPS) Instrument-2016

[13] Arendt K, Krzaczek M, and Florczuk, J, Numerical analysis by FEM and analytical study of the dynamic thermal behavior of hollow bricks with different cavity concentration 2011 *International Journal of Thermal Sciences* **50**(8) 1543-53

[14] Guattari C, Evangelisti L, Gori P and Asdrubali F, Influence of internal heat sources on thermal resistance evaluation through the heat flow meter method 2017 *Energy and Buildings* **135** 187-200

[15]   Pasquale V, Solar irradiance in NW Italy 1987 *Theoretical and applied climatology* **38**(2) 85-92

[16]   Ghizdăveț Z, Ștefan B M, Nastac D, Vasile O and Bratu M, Sound absorbing materials made by embedding crumb rubber waste in a concrete matrix 2016 *Construction and Building Materials* **124** 755-63

[17]   Abu-Jdayil B, Mourad A H and Hussain A, Thermal and physical characteristics of polyester–scrap tire composites 2006 *Construction and Building Materials* **105** 472-79

[18]   Owens P, Newman J and Choo B S 2003 *Advanced Concrete Technology Processes*, 1st ed. Oxford, U.K.: Elsevier Ltd., 2003, chapter 2 pp 72-74.